

Measurement of exclusive $\Upsilon(1S)$ and $\Upsilon(2S)$ decays into Vector-Pseudoscalar final states

C. P. Shen,^{2,35} C. Z. Yuan,¹⁸ I. Adachi,¹³ H. Aihara,⁶⁰ D. M. Asner,⁴⁶ V. Aulchenko,⁴ A. M. Bakich,⁵⁴ A. Bala,⁴⁷ B. Bhuyan,¹⁶ M. Bischofberger,³⁷ A. Bozek,⁴¹ M. Bračko,^{31,23} T. E. Browder,¹² V. Chekelian,³² A. Chen,³⁸ P. Chen,⁴⁰ B. G. Cheon,¹¹ K. Chilikin,²² I.-S. Cho,⁶⁸ K. Cho,²⁶ V. Chobanova,³² Y. Choi,⁵³ D. Cinabro,⁶⁶ J. Dalseno,^{32,56} M. Danilov,^{22,34} J. Dingfelder,³ Z. Doležal,⁵ Z. Drásal,⁵ A. Drutskoy,^{22,34} D. Dutta,¹⁶ K. Dutta,¹⁶ S. Eidelman,⁴ D. Epifanov,⁶⁰ H. Farhat,⁶⁶ J. E. Fast,⁴⁶ T. Ferber,⁷ A. Frey,¹⁰ V. Gaur,⁵⁵ N. Gabyshev,⁴ S. Ganguly,⁶⁶ R. Gillard,⁶⁶ Y. M. Goh,¹¹ B. Golob,^{30,23} J. Haba,¹³ T. Hara,¹³ K. Hayasaka,³⁶ H. Hayashii,³⁷ Y. Hoshi,⁵⁸ W.-S. Hou,⁴⁰ H. J. Hyun,²⁸ T. Iijima,^{36,35} A. Ishikawa,⁵⁹ R. Itoh,¹³ Y. Iwasaki,¹³ T. Julius,³³ D. H. Kah,²⁸ J. H. Kang,⁶⁸ E. Kato,⁵⁹ T. Kawasaki,⁴³ C. Kiesling,³² D. Y. Kim,⁵² H. J. Kim,²⁸ J. B. Kim,²⁷ J. H. Kim,²⁶ K. T. Kim,²⁷ Y. J. Kim,²⁶ K. Kinoshita,⁶ J. Klucar,²³ B. R. Ko,²⁷ P. Kodyš,⁵ S. Korpar,^{31,23} P. Križan,^{30,23} P. Krokovny,⁴ T. Kumita,⁶² A. Kuzmin,⁴ Y.-J. Kwon,⁶⁸ S.-H. Lee,²⁷ R. Leitner,⁵ J. Li,⁵¹ Y. Li,⁶⁵ J. Libby,¹⁷ C. Liu,⁵⁰ Y. Liu,⁶ Z. Q. Liu,¹⁸ D. Liventsev,¹³ P. Lukin,⁴ D. Matvienko,⁴ K. Miyabayashi,³⁷ H. Miyata,⁴³ G. B. Mohanty,⁵⁵ A. Moll,^{32,56} T. Mori,³⁵ N. Muramatsu,⁴⁹ R. Mussa,²¹ Y. Nagasaka,¹⁴ E. Nakano,⁴⁵ M. Nakao,¹³ Z. Natkaniec,⁴¹ M. Nayak,¹⁷ E. Nedelkowska,³² C. Ng,⁶⁰ N. K. Nisar,⁵⁵ S. Nishida,¹³ O. Nitoh,⁶³ S. Ogawa,⁵⁷ S. Okuno,²⁴ S. L. Olsen,⁵¹ W. Ostrowicz,⁴¹ P. Pakhlov,^{22,34} C. W. Park,⁵³ H. Park,²⁸ H. K. Park,²⁸ T. K. Pedlar,⁶⁹ T. Peng,⁵⁰ R. Pestotnik,²³ M. Petrič,²³ L. E. Piilonen,⁶⁵ M. Ritter,³² M. Röhrken,²⁵ A. Rostomyan,⁷ S. Ryu,⁵¹ H. Sahoo,¹² T. Saito,⁵⁹ Y. Sakai,¹³ S. Sandilya,⁵⁵ L. Santelj,²³ T. Sanuki,⁵⁹ Y. Sato,⁵⁹ V. Savinov,⁴⁸ O. Schneider,²⁹ G. Schnell,^{1,15} C. Schwanda,¹⁹ K. Senyo,⁶⁷ O. Seon,³⁵ M. Shapkin,²⁰ V. Shebalin,⁴ T.-A. Shibata,⁶¹ J.-G. Shiu,⁴⁰ B. Shwartz,⁴ A. Sibidanov,⁵⁴ F. Simon,^{32,56} P. Smerkol,²³ Y.-S. Sohn,⁶⁸ A. Sokolov,²⁰ E. Solovieva,²² S. Stanič,⁴⁴ M. Starič,²³ M. Steder,⁷ M. Sumihama,⁹ T. Sumiyoshi,⁶² U. Tamponi,^{21,64} K. Tanida,⁵¹ G. Tatishvili,⁴⁶ Y. Teramoto,⁴⁵ T. Tsuboyama,¹³ M. Uchida,⁶¹ S. Uehara,¹³ Y. Unno,¹¹ S. Uno,¹³ P. Urquijo,³ S. E. Vahsen,¹² C. Van Hulse,¹ P. Vanhoefer,³² G. Varner,¹² V. Vorobyev,⁴ M. N. Wagner,⁸ C. H. Wang,³⁹ P. Wang,¹⁸ X. L. Wang,⁶⁵ M. Watanabe,⁴³ Y. Watanabe,²⁴ E. Won,²⁷ H. Yamamoto,⁵⁹ J. Yamaoka,¹² Y. Yamashita,⁴² S. Yashchenko,⁷ Y. Yook,⁶⁸ Y. Yusa,⁴³ C. C. Zhang,¹⁸ Z. P. Zhang,⁵⁰ V. Zhilich,⁴ and A. Zupanc²⁵

(The Belle Collaboration)

¹University of the Basque Country UPV/EHU, 48080 Bilbao

²Beihang University, Beijing 100191

³University of Bonn, 53115 Bonn

⁴Budker Institute of Nuclear Physics SB RAS and Novosibirsk State University, Novosibirsk 630090

⁵Faculty of Mathematics and Physics, Charles University, 121 16 Prague

⁶University of Cincinnati, Cincinnati, Ohio 45221

⁷Deutsches Elektronen-Synchrotron, 22607 Hamburg

⁸Justus-Liebig-Universität Gießen, 35392 Gießen

⁹Gifu University, Gifu 501-1193

¹⁰II. Physikalisches Institut, Georg-August-Universität Göttingen, 37073 Göttingen

¹¹Hanyang University, Seoul 133-791

¹²University of Hawaii, Honolulu, Hawaii 96822

¹³High Energy Accelerator Research Organization (KEK), Tsukuba 305-0801

¹⁴Hiroshima Institute of Technology, Hiroshima 731-5193

¹⁵Ikerbasque, 48011 Bilbao

¹⁶Indian Institute of Technology Guwahati, Assam 781039

¹⁷Indian Institute of Technology Madras, Chennai 600036

¹⁸Institute of High Energy Physics, Chinese Academy of Sciences, Beijing 100049

¹⁹Institute of High Energy Physics, Vienna 1050

²⁰Institute for High Energy Physics, Protvino 142281

²¹INFN - Sezione di Torino, 10125 Torino

²²Institute for Theoretical and Experimental Physics, Moscow 117218

²³J. Stefan Institute, 1000 Ljubljana

²⁴Kanagawa University, Yokohama 221-8686

²⁵Institut für Experimentelle Kernphysik, Karlsruher Institut für Technologie, 76131 Karlsruhe

²⁶Korea Institute of Science and Technology Information, Daejeon 305-806

²⁷Korea University, Seoul 136-713

²⁸Kyungpook National University, Daegu 702-701

²⁹École Polytechnique Fédérale de Lausanne (EPFL), Lausanne 1015

³⁰Faculty of Mathematics and Physics, University of Ljubljana, 1000 Ljubljana

- ³¹University of Maribor, 2000 Maribor
³²Max-Planck-Institut für Physik, 80805 München
³³School of Physics, University of Melbourne, Victoria 3010
³⁴Moscow Physical Engineering Institute, Moscow 115409
³⁵Graduate School of Science, Nagoya University, Nagoya 464-8602
³⁶Kobayashi-Maskawa Institute, Nagoya University, Nagoya 464-8602
³⁷Nara Women's University, Nara 630-8506
³⁸National Central University, Chung-li 32054
³⁹National United University, Miao Li 36003
⁴⁰Department of Physics, National Taiwan University, Taipei 10617
⁴¹H. Niewodniczanski Institute of Nuclear Physics, Krakow 31-342
⁴²Nippon Dental University, Niigata 951-8580
⁴³Niigata University, Niigata 950-2181
⁴⁴University of Nova Gorica, 5000 Nova Gorica
⁴⁵Osaka City University, Osaka 558-8585
⁴⁶Pacific Northwest National Laboratory, Richland, Washington 99352
⁴⁷Panjab University, Chandigarh 160014
⁴⁸University of Pittsburgh, Pittsburgh, Pennsylvania 15260
⁴⁹Research Center for Electron Photon Science, Tohoku University, Sendai 980-8578
⁵⁰University of Science and Technology of China, Hefei 230026
⁵¹Seoul National University, Seoul 151-742
⁵²Soongsil University, Seoul 156-743
⁵³Sungkyunkwan University, Suwon 440-746
⁵⁴School of Physics, University of Sydney, NSW 2006
⁵⁵Tata Institute of Fundamental Research, Mumbai 400005
⁵⁶Excellence Cluster Universe, Technische Universität München, 85748 Garching
⁵⁷Toho University, Funabashi 274-8510
⁵⁸Tohoku Gakuin University, Tagajo 985-8537
⁵⁹Tohoku University, Sendai 980-8578
⁶⁰Department of Physics, University of Tokyo, Tokyo 113-0033
⁶¹Tokyo Institute of Technology, Tokyo 152-8550
⁶²Tokyo Metropolitan University, Tokyo 192-0397
⁶³Tokyo University of Agriculture and Technology, Tokyo 184-8588
⁶⁴University of Torino, 10124 Torino
⁶⁵CNP, Virginia Polytechnic Institute and State University, Blacksburg, Virginia 24061
⁶⁶Wayne State University, Detroit, Michigan 48202
⁶⁷Yamagata University, Yamagata 990-8560
⁶⁸Yonsei University, Seoul 120-749
⁶⁹Luther College, Decorah, Iowa 52101

Using samples of 102 million $\Upsilon(1S)$ and 158 million $\Upsilon(2S)$ events collected with the Belle detector, we study exclusive hadronic decays of these two bottomonium resonances to $K_S^0 K^+ \pi^-$ and charge-conjugate (c.c.) states, $\pi^+ \pi^- \pi^0 \pi^0$, and $\pi^+ \pi^- \pi^0$, and to the two-body Vector-Pseudoscalar ($K^*(892)^0 \bar{K}^0 + \text{c.c.}$, $K^*(892)^- K^+ + \text{c.c.}$, $\omega \pi^0$, and $\rho \pi$) final states. For the first time, signals are observed in the modes $\Upsilon(1S) \rightarrow K_S^0 K^+ \pi^- + \text{c.c.}$, $\pi^+ \pi^- \pi^0 \pi^0$, and $\Upsilon(2S) \rightarrow \pi^+ \pi^- \pi^0 \pi^0$, and evidence is found for the modes $\Upsilon(1S) \rightarrow \pi^+ \pi^- \pi^0$, $K^*(892)^0 \bar{K}^0 + \text{c.c.}$, and $\Upsilon(2S) \rightarrow K_S^0 K^+ \pi^- + \text{c.c.}$ Branching fractions are measured for all the processes, while 90% confidence level upper limits on the branching fractions are also set for the modes with a statistical significance of less than 3σ . The ratios of the branching fractions of $\Upsilon(2S)$ and $\Upsilon(1S)$ decays into the same final state are used to test a perturbative QCD prediction for OZI-suppressed bottomonium decays.

PACS numbers: 13.25.Gv, 14.40.Pq, 12.38.Qk

The $\Upsilon(1S)$ and $\Upsilon(2S)$ are expected to decay mainly via three gluons, with a few percent probability to two gluons and a photon [1]. The two- and three-gluon channels provide an entry to many potential final states, including states made of pure glue (glueballs), light Higgs bosons, and states made of light quarks. The study of $\Upsilon(1S)$ and $\Upsilon(2S)$ hadronic decays may pave the way for a more complete understanding of how gluon final states fragment into hadrons. However, little experimental information is

available on exclusive decays of the Υ resonances below $B\bar{B}$ threshold. Recently, a few Vector-Tensor (VT) and Axial-vector-Pseudoscalar states from $\Upsilon(1S)$ and $\Upsilon(2S)$ decays were measured by the Belle Collaboration [2].

Perturbative quantum chromodynamics (pQCD) provides a relation for the ratios of the branching fractions (\mathcal{B}) for the OZI (Okubo-Zweig-Iizuka) [3] suppressed J/ψ

and $\psi(2S)$ decays to hadrons [4]

$$Q_\psi = \frac{\mathcal{B}_{\psi(2S) \rightarrow \text{hadrons}}}{\mathcal{B}_{J/\psi \rightarrow \text{hadrons}}} = \frac{\mathcal{B}_{\psi(2S) \rightarrow e^+e^-}}{\mathcal{B}_{J/\psi \rightarrow e^+e^-}} \approx 12\%, \quad (1)$$

which is referred to as the “12% rule” and is expected to apply with reasonable accuracy to both inclusive and exclusive decays. However, substantial deviations are seen for $\rho\pi$ and other Vector-Pseudoscalar (VP) final states such as $K^*(892)\bar{K}$, as well as for VT final states [5]. This is the so-called “ $\rho\pi$ puzzle.” None of the many existing theoretical explanations that have been proposed have been able to accommodate all of the measurements reported to date [6].

A similar rule can be derived for OZI-suppressed bottomonium decays, where we expect

$$Q_\Upsilon = \frac{\mathcal{B}_{\Upsilon(2S) \rightarrow \text{hadrons}}}{\mathcal{B}_{\Upsilon(1S) \rightarrow \text{hadrons}}} = \frac{\mathcal{B}_{\Upsilon(2S) \rightarrow e^+e^-}}{\mathcal{B}_{\Upsilon(1S) \rightarrow e^+e^-}} = 0.77 \pm 0.07. \quad (2)$$

This rule should hold better than the 12% rule for charmonium decay since the bottomonium states have higher mass and pQCD and the potential models have better predictive power, as has been demonstrated in calculations of the $b\bar{b}$ meson spectrum. For the $\pi^+\pi^-\pi^0$ and $\rho\pi$ modes, upper limits of 1.84×10^{-5} and 2×10^{-4} have been published [7] for the decays $\Upsilon(1S) \rightarrow \pi^+\pi^-\pi^0$ and $\Upsilon(1S) \rightarrow \rho\pi$, respectively.

If violation of the pQCD rules is observed in the bottomonium system, a comparison with the charmonium system may help to develop a theoretical explanation of the $\rho\pi$ puzzle. For $K^*(892)\bar{K}$, there is a large isospin-violating difference between the branching fractions for the charged and neutral $\psi(2S) \rightarrow K^*(892)\bar{K}$ decays; this is not seen in J/ψ decays [1]. This pattern can be probed in $\Upsilon(1S)$ and $\Upsilon(2S)$ decays.

In this paper, we report studies of exclusive hadronic decays of the $\Upsilon(1S)$ and $\Upsilon(2S)$ resonances to the $K_S^0 K^+ \pi^-$ [8], $\pi^+ \pi^- \pi^0 \pi^0$, and $\pi^+ \pi^- \pi^0$, and two-body VP ($K^*(892)^0 \bar{K}^0$, $K^*(892)^- K^+$, $\omega \pi^0$, and $\rho\pi$) final states. The data are collected with the Belle detector [9] operating at the KEKB asymmetric-energy e^+e^- collider [10]. This analysis is based on a 5.7 fb^{-1} $\Upsilon(1S)$ data sample (102 million $\Upsilon(1S)$ events), a 24.7 fb^{-1} $\Upsilon(2S)$ data sample (158 million $\Upsilon(2S)$ events) [11], and a 89.4 fb^{-1} continuum data sample collected at $\sqrt{s} = 10.52 \text{ GeV}$. Here, \sqrt{s} is the center-of-mass (C.M.) energy of the colliding e^+e^- system. The numbers of the $\Upsilon(1S)$ and $\Upsilon(2S)$ events are determined by counting the hadronic events in the data taken at the $\Upsilon(1S)$ and $\Upsilon(2S)$ peaks after subtracting the appropriately scaled continuum background from the data sample collected at $\sqrt{s} = 9.43 \text{ GeV}$ and 9.993 GeV , respectively. The selection criteria for hadronic events are validated with the off-resonance data by comparing the measured R value ($R = \frac{\sigma(e^+e^- \rightarrow \text{hadrons})}{\sigma(e^+e^- \rightarrow \mu^+\mu^-)}$) with CLEO’s result [12].

The EVTGEN [13] generator is used to simulate Monte Carlo (MC) events. For two-body decays, the angular distributions are generated using the formulae in Ref. [14]. Inclusive $\Upsilon(1S)$ and $\Upsilon(2S)$ MC events, produced using PYTHIA [15] with four times the luminosity of the real data, are used to identify possible peaking backgrounds from $\Upsilon(1S)$ and $\Upsilon(2S)$ decays.

The Belle detector is described in detail elsewhere [9]. It is a large-solid-angle magnetic spectrometer that consists of a silicon vertex detector (SVD), a 50-layer central drift chamber (CDC), an array of aerogel threshold Cherenkov counters (ACC), a barrel-like arrangement of time-of-flight scintillation counters (TOF), and an electromagnetic calorimeter comprised of CsI(Tl) crystals (ECL) located inside a superconducting solenoid coil that provides a 1.5 T magnetic field. An iron flux return located outside of the coil is instrumented to detect K_L^0 mesons and to identify muons (KLM).

For each charged track other than those from K_S^0 decays, the impact parameters perpendicular to and along the beam direction with respect to the interaction point are required to be less than 0.5 cm and 4 cm, respectively, and the transverse momentum must exceed 0.1 GeV/ c in the laboratory frame. Well-measured charged tracks are selected and the number of good charged tracks must equal four for the $K_S^0 K^+ \pi^-$ final state or two for the $\pi^+ \pi^- \pi^0 \pi^0$ and $\pi^+ \pi^- \pi^0$ final states. For each charged track, a likelihood \mathcal{L}_X is formed from several detector subsystems for particle hypothesis $X \in \{e, \mu, \pi, K, p\}$. A track with a likelihood ratio $\mathcal{R}_K = \frac{\mathcal{L}_K}{\mathcal{L}_K + \mathcal{L}_\pi} > 0.6$ is identified as a kaon, while a track with $\mathcal{R}_K < 0.4$ is treated as a pion [16]. With this selection, the kaon (pion) identification efficiency is about 85% (89%), while 6% (9%) of kaons (pions) are misidentified as pions (kaons). Similar likelihood ratios \mathcal{R}_e and \mathcal{R}_μ are defined to identify electrons and muons, respectively [17, 18].

Except for the $\pi^+ \pi^-$ pair from K_S^0 decay, all charged tracks are required to be positively identified as pions or kaons. The requirements $\mathcal{R}_\mu < 0.95$ and $\mathcal{R}_e < 0.95$ for the charged tracks remove 9.3% (79%) of the backgrounds for $K_S^0 K^+ \pi^-$ ($\pi^+ \pi^- \pi^0$) with no loss in efficiency.

For K_S^0 candidates decaying into $\pi^+ \pi^-$ in the $K_S^0 K^+ \pi^-$ mode, we require that the invariant mass of the $\pi^+ \pi^-$ pair lies within a $\pm 8 \text{ MeV}/c^2$ interval around the K_S^0 nominal mass (which contains about 95% of the signal according to MC simulation) and that the pair has a displaced vertex and flight direction consistent with a K_S^0 originating from the interaction point [19].

To be identified as a photon candidate, a cluster in the electromagnetic calorimeter should not match the extrapolated position of any charged track and should have energy exceeding 100 (200) MeV in the $\pi^+ \pi^- \pi^0 \pi^0$ ($\pi^+ \pi^- \pi^0$) mode. A π^0 candidate is reconstructed from a pair of photons. We perform a mass-constrained fit to the selected π^0 candidate and require $\chi^2 < 15$.

To remove additional backgrounds in the $\pi^+\pi^-\pi^0$ final state, we require a matching ECL cluster for each charged track, with $E_\pi^{\text{ECL}}/P_\pi > 0.02$. Here, E_π^{ECL} and P_π represent the energy deposited in the ECL and the momentum in the laboratory frame, respectively, for the pion candidate. To suppress the background events from the initial-state-radiation (ISR) process $e^+e^- \rightarrow \rho^0 \rightarrow \pi^+\pi^-$ where the charged tracks are combined with a π^0 candidate, we require $|(E_1 - E_2)/(E_1 + E_2)| < 0.65$, where E_1 and E_2 are the π^0 daughter-photon energies in the laboratory frame. To suppress background from the ISR process $e^+e^- \rightarrow \omega \rightarrow \pi^+\pi^-\pi^0$, the same requirement is imposed for the higher-momentum π^0 in the $\omega\pi^0$ mode.

We define an energy conservation variable $X_T = \Sigma_h E_h/\sqrt{s}$, where E_h is the energy of the final-state particle h in the e^+e^- C.M. frame. For signal candidates, X_T should be around 1. Figure 1 shows the X_T distributions for $\Upsilon(1S)$ and $\Upsilon(2S)$ decays to $K_S^0 K^+\pi^-$, $\pi^+\pi^-\pi^0\pi^0$, and $\pi^+\pi^-\pi^0$ after applying all selection criteria. Solid points with error bars are from data at the indicated Υ resonance.

The continuum background contribution is measured by extrapolating the data at $\sqrt{s} = 10.52$ GeV to the $\Upsilon(1S)$ and $\Upsilon(2S)$ resonances. For the extrapolation, we use the scale factor, $f_{\text{scale}} = \frac{\mathcal{L}_\Upsilon}{\mathcal{L}_{\text{con}}} \frac{\sigma_\Upsilon}{\sigma_{\text{con}}} \frac{\epsilon_\Upsilon}{\epsilon_{\text{con}}}$, where $\frac{\mathcal{L}_\Upsilon}{\mathcal{L}_{\text{con}}}$, $\frac{\sigma_\Upsilon}{\sigma_{\text{con}}}$ and $\frac{\epsilon_\Upsilon}{\epsilon_{\text{con}}}$ are the ratios of luminosity, cross sections and efficiencies, respectively, at the bottomonium masses and continuum energy points. For nominal results, the s dependence of the cross section is assumed to be $1/s^3$ [20] and the corresponding scale factor is about 0.12 for the $\Upsilon(1S)$ and 0.37 for the $\Upsilon(2S)$. The dependence of the cross section on the beam energy could vary from $1/s^3$ to $1/s^4$ [20, 21]; this range is included as a systematic uncertainty.

Besides the continuum background contribution, we search for possible backgrounds from $\Upsilon(1S)$ and $\Upsilon(2S)$ decays. No peaking backgrounds from the $\Upsilon(1S)$ and $\Upsilon(2S)$ inclusive MC samples are found in the X_T signal regions. Potential backgrounds due to particle misidentification — for example, from $2(\pi^+\pi^-)$ and $K^+K^-\pi^+\pi^-$ for $K_S^0 K^+\pi^-$ — are estimated and found to be negligible. In the lower X_T region, backgrounds arise from decays with additional π^0 's: from are $K_S^0 K^+\pi^-\pi^0$ for $K_S^0 K^+\pi^-$, $\pi^+\pi^-\pi^0\pi^0$ for $\pi^+\pi^-\pi^0\pi^0$, and $\pi^+\pi^-\pi^0\pi^0$ for $\pi^+\pi^-\pi^0$. There are also some backgrounds from $\tau^+\tau^- \rightarrow \pi^+\pi^-n\pi^0\nu_\tau\bar{\nu}_\tau$ with $n \geq 2$ for $\pi^+\pi^-\pi^0\pi^0$, and $n \geq 1$ for $\pi^+\pi^-\pi^0$. The X_T distributions from the above backgrounds are checked with MC simulations and found to be featureless.

We find that these backgrounds from $\Upsilon(1S)$ and $\Upsilon(2S)$ decays together with the normalized contribution from continuum production can describe the data in the $X_T < 0.975$ region very well. For $\pi^+\pi^-\pi^0\pi^0$ ($\pi^+\pi^-\pi^0$), the fraction of events with multiple combinations is 2.1% (1.7%) due to multiple π^0 candidates; this is consistent with the MC simulation and is taken into account in the

efficiency determination.

An unbinned simultaneous maximum likelihood fit to the X_T distributions is performed to extract the signal and background yields in the $\Upsilon(1S)$ and continuum data samples, and in the $\Upsilon(2S)$ and continuum data samples. The signal shapes are obtained from MC simulated signal samples directly, where for $K_S^0 K^+\pi^-$ the signal shape is smeared with a Gaussian function to account for an 18% difference in the resolution between data and MC samples. In this fit, an exponential background shape is used for the $\Upsilon(1S)/\Upsilon(2S)$ decay backgrounds in addition to the normalized continuum contribution. The fit ranges and results for the X_T distributions from $K_S^0 K^+\pi^-$, $\pi^+\pi^-\pi^0\pi^0$, and $\pi^+\pi^-\pi^0$ candidate events are shown in Fig. 1, and the fit results are summarized in Table I.

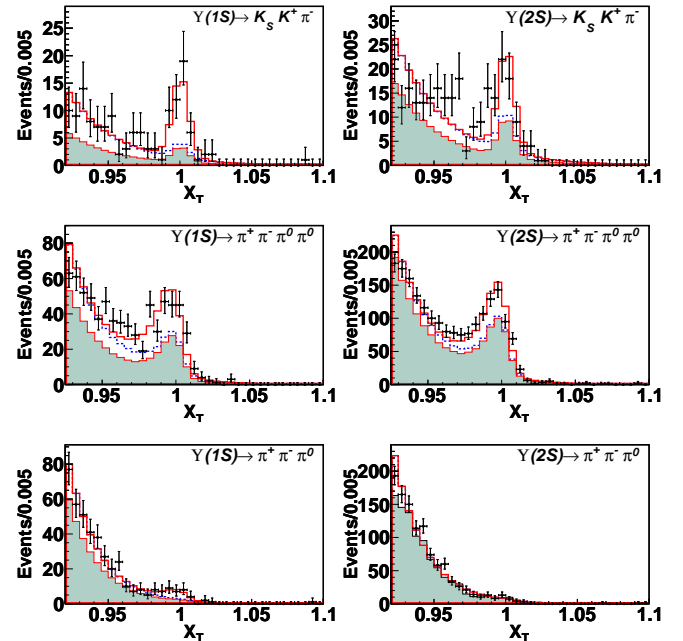


FIG. 1: The fits to the scaled total energy X_T distributions from $\Upsilon(1S)$ and $\Upsilon(2S)$ decays to $K_S^0 K^+\pi^-$, $\pi^+\pi^-\pi^0\pi^0$, and $\pi^+\pi^-\pi^0$. Solid points with error bars are from resonance data. The solid histograms show the best fits, dashed curves are the total background estimates, and shaded histograms are the normalized continuum background contributions.

We determine a Bayesian 90% confidence level (C.L.) upper limit on N_{sig} by finding the value $N_{\text{sig}}^{\text{UL}}$ such that $\int_0^{N_{\text{sig}}^{\text{UL}}} \mathcal{L} dN_{\text{sig}} = 0.90$, where N_{sig} is the number of signal events and \mathcal{L} is the value of the likelihood as a function of N_{sig} . The statistical significance of the signal is estimated from the difference of the logarithmic likelihoods, $-2 \ln(\mathcal{L}_0/\mathcal{L}_{\text{max}})$, taking into account the difference in the number of degrees of freedom in the fits, where \mathcal{L}_0 and \mathcal{L}_{max} are the likelihoods of the fits without and with signal, respectively.

After requiring the value of the variable $|X_T - 1|$ to be less than 0.02 for $K_S^0 K^+\pi^-$ and less than 0.025

for $\pi^+\pi^-\pi^0\pi^0$ and $\pi^+\pi^-\pi^0$, the Dalitz plots for the $K_S^0 K^+ \pi^-$ and $\pi^+\pi^-\pi^0$ final states and the scatter plot of $M(\pi^+\pi^-\pi_l^0)$ versus $M(\pi^+\pi^-\pi_h^0)$ for the $\pi^+\pi^-\pi_h^0\pi_l^0$ final state are shown in Fig. 2. In the scatter plot, π_h^0 and π_l^0 represent the pion with a higher and lower momentum in the laboratory system, respectively. According to MC simulated $\Upsilon \rightarrow \omega\pi^0$ signal events, over 97% of the π^0 s from ω decays have the lower momentum and there is only one $\pi^+\pi^-\pi^0$ combination in the ω mass region.

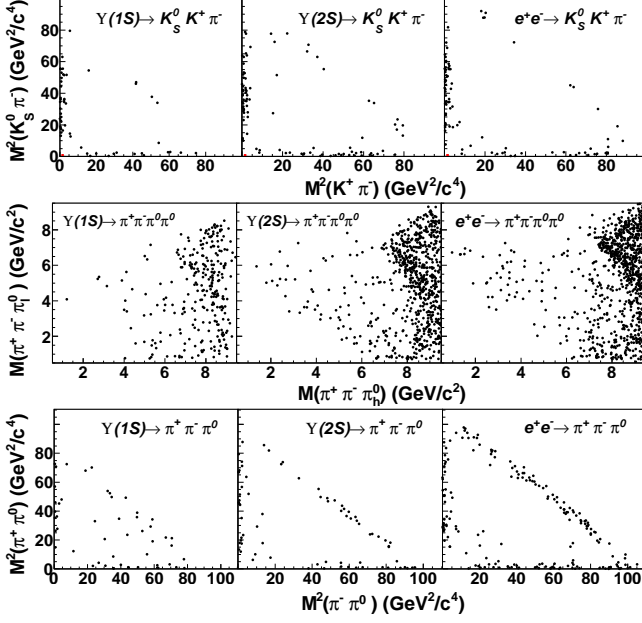


FIG. 2: Dalitz plots for the $K_S^0 K^+ \pi^-$ (top row) and $\pi^+\pi^-\pi^0$ (bottom row) final states, and scatter plot for the $\pi^+\pi^-\pi^0\pi^0$ (middle row) final state. Here, the left column is for $\Upsilon(1S)$ decays, the middle column is for $\Upsilon(2S)$ decays, and the right column is for the continuum data without normalization. In $\pi^+\pi^-\pi^0\pi^0$, π_h^0 and π_l^0 represent the pion with a higher and lower momentum in the laboratory system, respectively.

For the selected events, Fig. 3 shows the $K^+\pi^-$ and $K_S^0\pi^-$ invariant mass distributions for the $K_S^0 K^+ \pi^-$ final state, the $\pi^+\pi^-\pi^0$ invariant mass distribution for the $\pi^+\pi^-\pi^0\pi^0$ final state, and the $\pi\pi$ invariant mass distribution for the $\pi^+\pi^-\pi^0$ final state [22]. There are hints of the vector mesons $K^*(892)^0$, $K^*(892)^-$, ω , and ρ in the expected mass regions, but except for possible evidence for a $K^*(892)^0$ signal from $\Upsilon(1S)$ decays, there is no indication of signal in any other final state.

We perform a similar unbinned simultaneous maximum likelihood fit described above for X_T distributions, except that a first-order Chebyshev polynomial is used instead of the exponential background shape. Because of the limited statistics, in the fits we assume there is no interference between the vector meson signal and other non-resonant components. We also neglect the possible small interference between the Υ resonance decays and continuum process due to the narrow widths of the Υ resonances. The results of the fits are shown in Fig. 3

and listed in Table I.

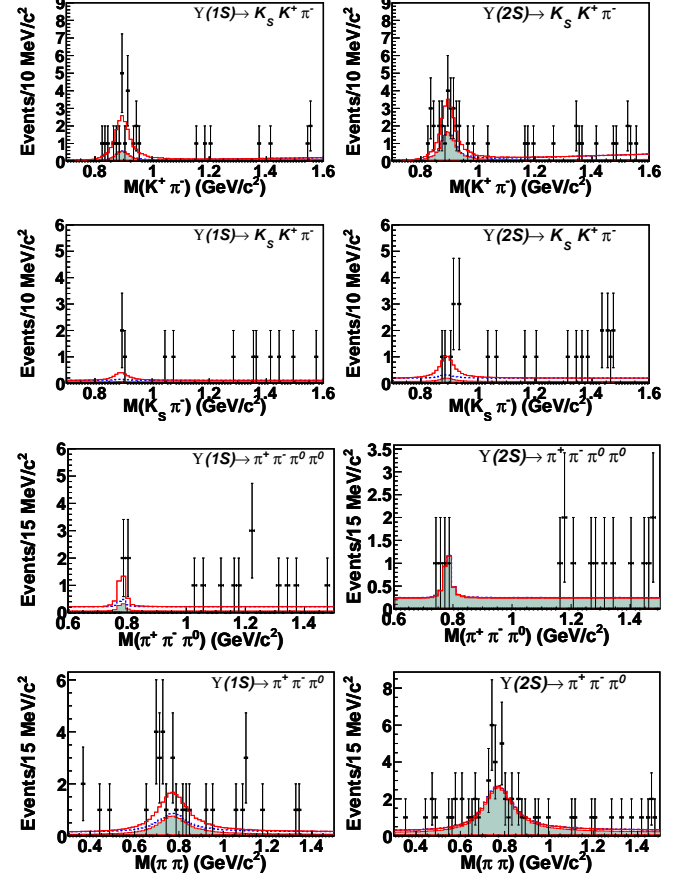


FIG. 3: The fits to the $K^+\pi^-$, $K_S^0\pi^-$, $\pi^+\pi^-\pi^0$ and $\pi\pi$ mass distributions for the $K^*(892)^0$, $K^*(892)^-$, ω and ρ vector meson candidates from $K_S^0 K^+ \pi^-$, $\pi^+\pi^-\pi^0\pi^0$ and $\pi^+\pi^-\pi^0$ events from $\Upsilon(1S)$ and $\Upsilon(2S)$ decays (VP modes). The solid histograms show the results of the simultaneous fits, the dotted curves show the total background estimates, and the shaded histograms are the normalized continuum contributions.

There are several sources of systematic errors for the branching fraction measurements. The uncertainty in the tracking efficiency for tracks with angles and momenta characteristic of signal events is about 0.35% per track and is additive. The uncertainty due to particle identification efficiency is 1.7% with an efficiency correction factor of 0.98 for each pion, and is 1.6% with an efficiency correction factor of 0.97 for each kaon. The uncertainty in selecting a π^0 candidate is estimated using a control sample of $\tau^- \rightarrow \pi^-\pi^0\nu_\tau$ events. We include a 2.2% systematic error with efficiency correction factors of 0.94 for low-momentum and 0.97 for high-momentum π^0 mesons. In the $K_S^0 K^+ \pi^-$ mode, the K_S^0 reconstruction and the systematic error is verified by comparing the ratio of $D^+ \rightarrow K_S^0 \pi^+$ and $D^+ \rightarrow K^- \pi^+ \pi^+$ yields with the MC expectations; the difference between data and MC simulation is less than 4.9% [23]. The efficiency of the requirement $E_\pi^{\text{ECL}}/P_\pi > 0.02$ is 97.4% in $\pi^+\pi^-\pi^0$ and

TABLE I: Results for the $\Upsilon(1S)$ and $\Upsilon(2S)$ decays, where N_{sig} is the number of signal events from the fits, $N_{\text{sig}}^{\text{UL}}$ is the upper limit on the number of signal events, ϵ is the efficiency (%), Σ is the statistical significance (in units of 10^{-6}), \mathcal{B} is the branching fraction (in units of 10^{-6}), \mathcal{B}^{UL} is the 90% C.L. upper limit on the branching fraction, Q_{Υ} is the ratio of the $\Upsilon(2S)$ and $\Upsilon(1S)$ branching fractions, and Q_{Υ}^{UL} is the upper limit on the value of Q_{Υ} . The first error in \mathcal{B} and Q_{Υ} is statistical, and the second systematic. Here $\mathcal{B}(K_S^0 \rightarrow \pi^+ \pi^-)$ has been included in the efficiency for the $K_S^0 K^+ \pi^-$ final states. In order to set conservative upper limits on these branching fractions, the efficiencies are lowered by a factor of $1 - \sigma_{\text{sys}}$ in the calculation, where σ_{sys} is the total systematic error.

Channel	$\Upsilon(1S)$				$\Upsilon(2S)$				Q_{Υ}	Q_{Υ}^{UL}				
	N_{sig}	$N_{\text{sig}}^{\text{UL}}$	ϵ	Σ	\mathcal{B}	\mathcal{B}^{UL}	N_{sig}	$N_{\text{sig}}^{\text{UL}}$			ϵ	Σ		
$K_S^0 K^+ \pi^-$	37.2 ± 7.6	—	22.96	6.2	$1.59 \pm 0.33 \pm 0.18$	—	39.5 ± 10.3	—	21.88	4.0	$1.14 \pm 0.30 \pm 0.13$	—	$0.72 \pm 0.24 \pm 0.09$	—
$\pi^+ \pi^- \pi^0 \pi^0$	143.2 ± 22.4	—	11.20	7.1	$12.8 \pm 2.01 \pm 2.27$	—	260.7 ± 37.2	—	12.98	7.4	$13.0 \pm 1.86 \pm 2.08$	—	$1.01 \pm 0.22 \pm 0.23$	—
$\pi^+ \pi^- \pi^0$	25.5 ± 8.6	—	11.86	3.4	$2.14 \pm 0.72 \pm 0.34$	—	-2.1 ± 9.5	15	13.19	—	$-0.10 \pm 0.46 \pm 0.02$	0.80	$-0.05 \pm 0.21 \pm 0.02$	0.42
$K^*(892)^0 K^0$	16.1 ± 4.7	—	16.23	4.4	$2.92 \pm 0.85 \pm 0.37$	—	14.7 ± 6.0	30	15.59	2.7	$1.79 \pm 0.73 \pm 0.30$	4.22	$0.61 \pm 0.31 \pm 0.12$	1.20
$K^*(892)^- K^+$	2.0 ± 1.9	6.3	18.92	1.3	$0.31 \pm 0.30 \pm 0.04$	1.11	5.7 ± 3.4	13	18.77	2.0	$0.58 \pm 0.35 \pm 0.09$	1.45	$1.87 \pm 2.12 \pm 0.33$	5.52
$\omega \pi^0$	2.5 ± 2.1	6.8	2.11	1.6	$1.32 \pm 1.11 \pm 0.14$	3.90	0.1 ± 2.2	4.6	2.32	0.1	$0.03 \pm 0.68 \pm 0.01$	1.63	$0.02 \pm 0.50 \pm 0.01$	1.68
$\rho \pi$	11.3 ± 5.9	22	6.41	2.2	$1.75 \pm 0.91 \pm 0.28$	3.68	-1.4 ± 8.6	14	8.66	—	$-0.11 \pm 0.64 \pm 0.03$	1.16	$-0.06 \pm 0.38 \pm 0.02$	0.94

the uncertainty can be neglected according to a check of the results with and without this requirement. Errors on the branching fractions of the intermediate states are taken from the PDG listings [1]. For the $\pi^+ \pi^- \pi^0$ final state, the trigger efficiency is verified using the pure ISR control sample $e^+ e^- \rightarrow \omega \rightarrow \pi^+ \pi^- \pi^0$. According to MC simulation, for the $\pi^+ \pi^- \pi^0$ ($\rho \pi$) mode, the trigger efficiency is 97% (94%), with an uncertainty that is smaller than 1.5% (3%); for the other modes, the trigger efficiency is greater than 99% and the corresponding uncertainty is neglected. The trigger efficiency in $\rho \pi$ is somewhat lower due to high momentum π^0 in $\rho^0 \pi^0$. We estimate the systematic errors associated with the fitting procedure by changing the order of the background polynomial, the range of the fit and introducing an extra Gaussian function to describe the possible excess around $X_T \sim 0.96$ in X_T fits and take the differences in the results of the fits, which are 1.5%-11% depending on the final state particles, as systematic errors. To investigate the effect of possible intermediate resonances for the $\Upsilon(1S)/\Upsilon(2S) \rightarrow K_S^0 K^+ \pi^-$, $\pi^+ \pi^- \pi^0 \pi^0$ and $\pi^+ \pi^- \pi^0$ decays, the efficiencies are estimated by using sampled phase space MC signal events according to the Dalitz plot or scatter plot that are shown in Fig. 2. The difference is 7.3%/5.3% for $\Upsilon(1S)/\Upsilon(2S) \rightarrow K_S^0 K^+ \pi^-$, 5.6%/4.4% for $\Upsilon(1S)/\Upsilon(2S) \rightarrow \pi^+ \pi^- \pi^0 \pi^0$, 11%/7.8% for $\Upsilon(1S)/\Upsilon(2S) \rightarrow \pi^+ \pi^- \pi^0$; these values are assigned as a systematic uncertainty due to this source. For the $K^*(892)\bar{K}$ and $\rho \pi$ modes, we estimate the systematic errors associated with the resonance parameters by changing the values of the masses and widths of the resonances by $\pm 1\sigma$. The $K^*(892)$ and ρ line shapes are replaced by a relativistic Breit-Wigner function and the Gounaris-Sakurai parametrization [24], respectively. The total differences of 2.6%-11% in the fitted results are taken as systematic errors. For the central values of the branching fractions, the difference between alternative C.M. energy dependences of the cross section is included as a systematic error due to the uncertainty of the continuum contribution, which is in the range of 4.7% to 22%. The uncertainty due to limited MC statistics is at most 2.7%. Finally, the uncertainties on the total numbers of $\Upsilon(1S)$ and $\Upsilon(2S)$ events are 2.2% and 2.3%, respectively, which are mainly due to imperfect simulations of the charged multiplicity distributions from inclusive hadronic MC events. Assuming that all of these systematic error sources are independent, the total systematic error is 11%-26% depending on the final state, as shown in Table II.

Table I shows the results for the branching fractions including the upper limits at 90% C.L. for the channels with a statistical significance of less than 3σ . In order to set conservative upper limits on these branching fractions, the efficiencies are lowered by a factor of $1 - \sigma_{\text{sys}}$ in the calculation, where σ_{sys} is the total systematic error. The corresponding ratio of the branching fractions

TABLE II: Relative systematic errors (%) on the decay branching fractions.

Source ($\Upsilon(1S)/\Upsilon(2S)$)	$K_S^0 K^+ \pi^-$	$\pi^+ \pi^- \pi^0 \pi^0$	$\pi^+ \pi^- \pi^0$	$K^*(892)^0 K^0$	$K^*(892)^- K^+$	$\omega \pi^0$	$\rho \pi$
Tracking	0.7	0.7	0.7	0.7	0.7	0.7	0.7
PID	3.3	3.4	3.4	3.3	3.3	3.4	3.4
π^0 selection	—	4.4	2.2	—	—	4.4	2.2
K_S^0 selection	4.9	—	—	4.9	4.9	—	—
Branching fractions	0.1	0.1	0.1	0.1	0.1	0.8	0.1
Trigger	—	—	1.5	—	—	—	3.0
Fitting procedure	1.5/3.4	3.7/5.6	9.3/9.5	8.0/11	9.4/11	4.9/11	3.2/5.3
Intermediate resonance	7.3/5.3	5.6/4.4	11/7.8	—	—	—	—
Resonance parametrization	—	—	—	2.6/3.8	4.0/6.2	—	4.6/11
Continuum uncertainty	4.7/4.7	15/12	4.7/12	6.5/9.4	3.7/1.4	6.8/6.6	14/22
MC statistics	1.7/1.8	2.7/2.5	0.9/0.8	2.2/2.3	2.1/2.1	2.0/1.9	0.9/0.8
Number of Υ events	2.2/2.3	2.2/2.3	2.2/2.3	2.2/2.3	2.2/2.3	2.2/2.3	2.2/2.3
Sum in quadrature	11/11	18/16	16/18	13/17	13/15	11/15	16/26

of $\Upsilon(2S)$ and $\Upsilon(1S)$ decay (Q_Υ) is calculated; in some cases, the systematic errors cancel. A Bayesian upper limit on the ratio at the 90% C.L. (Q_Υ^{UL}) is obtained by performing toy MC experiments. We sample $\mathcal{B}_{\Upsilon(1S)}$ and $\mathcal{B}_{\Upsilon(2S)}$ by assuming they follow Gaussian distributions, where the mean values and standard deviations of the Gaussian functions are set to be the central value and total error (with a common error removed) of the branching fraction, respectively. For the sampled distribution of the ratio of the branching fractions greater than zero, we obtain Q_Υ^{UL} , where Q_Υ^{UL} corresponds to the number of experiments with $Q_\Upsilon < Q_\Upsilon^{UL}$ in less than 90% of the total number of toy experiments. At present, all the results on the branching fractions, including upper limits reported in this letter, are the first measurements or the best measurements.

In summary, we have measured $\Upsilon(1S)$ and $\Upsilon(2S)$ exclusive hadronic decays to $K_S^0 K^+ \pi^-$, $\pi^+ \pi^- \pi^0 \pi^0$, and $\pi^+ \pi^- \pi^0$, as well as the two-body VP ($K^*(892)^0 \bar{K}^0$, $K^*(892)^- K^+$, $\omega \pi^0$, and $\rho \pi$) states. Signals are observed for the first time in the $\Upsilon(1S) \rightarrow K_S^0 K^+ \pi^-$, $\pi^+ \pi^- \pi^0 \pi^0$ and $\Upsilon(2S) \rightarrow \pi^+ \pi^- \pi^0 \pi^0$ decay modes. Although many $\Upsilon(1S)$ and $\Upsilon(2S)$ exclusive decay modes were previously measured using CLEO data [25], only the $K_S^0 K^+ \pi^-$ mode overlaps with our measurement and upper limits at 90% C.L. were presented there. Our results for the $K_S^0 K^+ \pi^-$ mode are well below the upper bounds reported in Ref. [25]. There is an indication for large isospin-violation between the branching fractions for the charged and neutral $K^*(892) \bar{K}$ for both $\Upsilon(1S)$ and $\Upsilon(2S)$ decays, as in $\psi(2S)$ decays, which indicates that the electromagnetic process plays an important role in these decays [26]. We find that, for the processes $K_S^0 K^+ \pi^-$ and $\pi^+ \pi^- \pi^0 \pi^0$, the Q_Υ ratios are consistent with the expected value; for $\pi^+ \pi^- \pi^0$, the Q_Υ ratio is a little lower than the pQCD prediction. The results for the other modes are inconclusive due to low statistical significance. These results may supply useful guidance for interpreting violations of the 12% rule for OZI-suppressed decays in the charmonium sector.

We thank the KEKB group for excellent operation

of the accelerator; the KEK cryogenics group for efficient solenoid operations; and the KEK computer group, the NII, and PNNL/EMSL for valuable computing and SINET4 network support. We acknowledge support from MEXT, JSPS and Nagoya's TLPSC (Japan); ARC and DIISR (Australia); FWF (Austria); NSFC (China); MSMT (Czechia); CZF, DFG, and VS (Germany); DST (India); INFN (Italy); MEST, NRF, GSDC of KISTI, and WCU (Korea); MNiSW and NCN (Poland); MES and RFAAE (Russia); ARRS (Slovenia); IKERBASQUE and UPV/EHU (Spain); SNSF (Switzerland); NSC and MOE (Taiwan); and DOE and NSF (USA).

-
- [1] J. Beringer *et al.* (Particle Data Group), Phys. Rev. D **86**, 010001 (2012).
 - [2] C. P. Shen *et al.* (Belle Collaboration), Phys. Rev. D **86**, 031102(R) (2012).
 - [3] S. Okubo, Phys. Lett. **5**, 165 (1963); G. Zweig, CERN Report Th 401 and 412 (1964); J. Iizuka, K. Okada, and O. Shito, Prog. Theor. Phys. **35**, 1061 (1966); J. Iizuka, Prog. Theor. Phys. Suppl. **37**, 21 (1966).
 - [4] T. Appelquist and H. D. Politzer, Phys. Rev. Lett. **34**, 43 (1975); A. De Rújula and S. L. Glashow, Phys. Rev. Lett. **34**, 46 (1975).
 - [5] M. E. B. Franklin *et al.*, Phys. Rev. Lett. **51**, 963 (1983); J. Z. Bai *et al.* (BES Collaboration), Phys. Rev. D **69**, 072001 (2004).
 - [6] For reviews, please see X. H. Mo, C. Z. Yuan and P. Wang, High Energy Phys. and Nucl. Phys. **31**, 686 (2007) [arXiv:hep-ph/0611214]; N. Brambilla *et al.*, Eur. Phys. J. C **71**, 1534 (2011); Y. F. Gu and X. H. Li, Phys. Rev. D **63**, 114019 (2001).
 - [7] R. Fulton *et al.* (CLEO Collaboration), Phys. Rev. D **41**, 1401 (1990); A. Anastassov *et al.* (CLEO Collaboration), Phys. Rev. Lett. **82**, 286 (1999).
 - [8] Charge-conjugate decays are implicitly assumed throughout the paper and the $\rho \pi$ mode includes $\rho^0 \pi^0$, $\rho^+ \pi^-$ and $\rho^- \pi^+$.
 - [9] A. Abashian *et al.* (Belle Collaboration), Nucl. Instrum. Methods Phys. Res., Sect. A **479**, 117 (2002); also see detector section in J. Brodzicka *et al.*, Prog. Theor. Exp. Phys. (2012) 04D001.

- [10] S. Kurokawa and E. Kikutani, Nucl. Instrum. Methods Phys. Res., Sect. A **499**, 1 (2003), and other papers included in this volume; T. Abe *et al.*, Prog. Theor. Exp. Phys. (2013) 03A001 and following articles up to 03A011.
- [11] X. L. Wang *et al.* (Belle Collaboration), Phys. Rev. D **84**, 071107(R) (2011).
- [12] D. Besson *et al.* (CLEO Collaboration), Phys. Rev. D **76**, 072008 (2010).
- [13] D. J. Lange, Nucl. Instrum. Methods Phys. Res., Sect. A **462**, 152 (2001).
- [14] Y. Tosa, DPNU-34-1976.
- [15] T. Sjöstrand, S. Mrenna and P. Skands, JHEP **026**, 0605 (2006).
- [16] E. Nakano, Nucl. Instrum. Methods Phys. Res., Sect. A **494**, 402 (2002).
- [17] K. Hanagaki *et al.*, Nucl. Instrum. Methods Phys. Res., Sect. A **485**, 490 (2002).
- [18] A. Abashian *et al.*, Nucl. Instrum. Methods Phys. Res., Sect. A **491**, 69 (2002).
- [19] F. Fang, Ph.D thesis, University of Hawaii, 2003 [<http://belle.kek.jp/bdocs/theses.html>].
- [20] K. Belous *et al.* (Belle Collaboration), Phys. Lett. B **681**, 400 (2009).
- [21] V. L. Chernyak and A. R. Zhitnitsky, Phys. Rept. **112**, 173 (1984); Cai-Dian Lü, Wei Wang and Yu-Ming Wang, Phys. Rev. D **75**, 094020 (2007).
- [22] The $\pi\pi$ invariant mass includes $\pi^+\pi^-$, $\pi^+\pi^0$ and $\pi^-\pi^0$ invariant masses.
- [23] S.-W. Lin *et al.* (Belle Collaboration), Phys. Rev. Lett. **99**, 121601 (2007).
- [24] G. J. Gounaris and J. J. Sakurai, Phys. Rev. Lett. **21**, 244 (1968).
- [25] S. Dobbs *et al.*, Phys. Rev. D **86**, 052003 (2012).
- [26] The ratio of cross sections between neutral and charged $K^*(892)\bar{K}$ is larger than 4.6 at 90% C.L. in continuum data sample at $\sqrt{s} = 10.52$ GeV, which is not very different from the expected value of 4 with the assumption of $SU(3)$ symmetry [27].
- [27] Cai-Dian Lü, Wei Wang and Yu-Ming Wang, Phys. Rev. D **75**, 094020 (2007).